

In Search of the True Interlaminar Shear Strength

PAOLO J. FERABOLI AND KEITH T. KEDWARD

ABSTRACT

The search for a practicable test method by which interlaminar shear (ILS) strength can be reliably measured has eluded the composites community for many years. Currently, the most widely practiced ILS strength standard is the three-point bend test ASTM D2344, also known as short beam shear (SBS). Many are the problems associated with such test method, such as the great deal of compressive stresses under the roller, the dependence of the “apparent” ILS strength on the support span to laminate thickness ratio (s/t), and the non pure shear state of stress, which affect the true measurement of the desired mechanical property. On the other hand the great advantage of this test method is its simplicity, and the ability of being performed rapidly and in much more reliable manner than other ILS strength test methods (such as Iosipescu and Double-notched tension), which involve complex fixtures or extensive machining. Furthermore, even these test methods have limitations associated with complexities in attaining a uniform state of interlaminar shear stress over a significant area.

In this paper a simple modification to the SBS specimen is evaluated, wherein the surface area of shear failure is reduced by introducing a longitudinal “notch”. An investigation based on an integrated experimental and analytical approach is performed to study the influence of groove dimensions on the measured ILS strength of a carbon/epoxy laminate. Among the advantages observed for this modified “Joshua” specimen, the reduced cross section at the midplane precipitates ILS failure at lower applied loads, and the relative independence of the results from the support span facilitates the use of more flexural configurations (greater s/t ratios). In turn, this modified I-beam-type specimen favors the adoption of a specimen geometry that is user-friendly, while obtaining a state of stress that is closer to pure shear, lowering the local and bending compressive stresses experienced by, and achieving better control on the location of failure initiation and propagation.

Keywords: short beam shear, interlaminar shear, delamination, testing.

[†] Department of Mechanical Engineering – University of California, Santa Barbara, CA 93106

[∞] Corresponding author, Tel: (805) 407 1123, E-mail: pmc@engineering.ucsb.edu

1. INTRODUCTION

An impediment to the wider and quicker exploitation of composite materials is their susceptibility to delamination damage. While the anisotropic nature of laminated composite materials can become a source of delamination, in most practical situations the lower matrix dominated properties, such as the through-thickness strength, with respect to in-plane properties makes them vulnerable to localized transverse forces, whether manufacturing or work related. In particular, highly detrimental interlaminar shear (ILS) stresses develop at local discontinuities such ply-drops, bonded and bolted joints, or during handling, assembly or foreign object impact. According to current literature, these stresses need to be evaluated for structural applications and many authors feel that delamination growth is the fundamental issue in the evaluation of laminated composite systems for durability and damage tolerance.

While a great deal of advancements has been accomplished in the recent years, there is not a universally accepted test method for characterizing a composite material's resistance to delamination. Furthermore, the concepts of interlaminar shear strength (τ_{ILS}) and interlaminar fracture toughness (G_{IIc}) are constantly questioned as being true material properties rather than test configuration-dependent properties [1,2].

Currently, the most widely accepted and practiced ILS strength standard is the three-point bend test ASTM D2344 [3], also known as short beam shear (SBS). Many are the problems associated with such test method [4-12]. The first cause of concern has always been the great deal of compressive stresses present underneath the loading roller, which are thought to act either as crack initiators or inhibitors. The stress distribution typical of hard-body to soft-surface contact is characterized by a "skewed" profile, which prevents from achieving pure and reproducible delamination damage, and it is characterized by a complex interaction of damage mechanisms, such as matrix cracking and local fiber breakage. The modified version of this test, which employs a four-point bend configuration, greatly reduces the extent of damage at the central contact location, but results in a less convenient geometry, particularly for dynamic testing.

Another fundamental source of concern on this test methodology arises due to the inability to introduce a pure shear state of stress. The bending moment contributes in the deformation of the coupon, therefore introducing undesired stress components inhibiting the true measurement of the desired mechanical property. While the four-point bend geometry can be adjusted to obtain a constant moment over a large portion of the specimen, the critical location for delamination initiation (remote from the loading rollers) is still subject to a complex stress state [4].

Finally, previous researchers investigated analytically and experimentally the influence of the support span to laminate thickness ratio (s/t) on test results, and concluded that the "apparent" ILS strength decreases with increasing span, and that small variations in test geometry can shift the failure modes, from shear to flexure dominated. On the other hand the value of $s/t = 4.0$ recommended by ASTM International often results in great experimental inconveniences, such as the need to machine and test very small specimens.

However, the great advantage of this test is its simplicity, and the ability of being performed rapidly and in much more reliable manner than other current ILS

strength test methods, which involve complex fixtures or extensive machining, and still exhibit limitations in attaining a uniform state of interlaminar shear stress over a significant area.

While improved material systems, design procedures, and through-thickness reinforcements are always on the horizon, a need for a reliable method for measuring the ILS strength exists. In order to benefit from all the advantages of this test method, while addressing and possibly resolving the related issues, a new specimen is here developed which uses the same three-point configuration as the aforementioned SBS.

From beam theory it is known that peak ILS occurs at the midplane of a beam loaded in three-point bending (once sufficiently away from the rollers, as later indicated in [fig. 8](#)), and it is inversely related to the specimen width and thickness. Accordingly, a reduction in cross sectional area (smaller specimen) should precipitate failure at the same applied stress but lower applied load. This would apply if the test were an accurate measurement of a true mechanical property. As mentioned above, this cannot be said for the SBS specimen, where coupon dimensions greatly affect the “apparent” interlaminar shear strength. This specimen, referred to as the Joshua specimen ([fig. 1](#)), takes its shape from traditional I-beam, which exhibits a short, thick flange and relatively wide web. The reduced cross section should then initiate failure at lower loads, thus reducing local compressive and global bending stresses, while becoming independent of specimen and test geometry thanks to the more pure state of stress acting in the critical zone around the midplane. Purpose of this paper is to establish reliable and convenient (economical) test method, while determining the influence of notch depth and height on the measured strength, in the effort of developing a standard that is simple to setup but achieves more precise assessment of the long-sought true interlaminar shear strength.

2. RESULTS

2.1 MATERIALS, SPECIMENS AND TEST GEOMETRY

The laminates are obtained by hand lay-up of AS4/NCT301 prepreg tape, press molded at 300°F (149°C) for 30 minutes at a pressure of 3 bars (43.5 psi). The stacking sequence is quasi-isotropic of the form $[0/90^\circ/\pm 45]_{4s}$, with a nominal ply thickness of 0.0045 in. (0.11 mm), giving nominal laminate thickness of 0.145 in. (3.68 mm). The elastic properties of the unidirectional lamina and quasi-isotropic laminate are summarized in [table I](#).

Specimens are machined from 12”x12” (304.8 x 304.8 mm) panels with a diamond coated tip disk saw. Strips of material approximately ¼ in. (6.35 mm) in width are cut from the plate boundary in order to minimize the influence of manufacturing related defects on test results. It has been previously assessed [4] that in specimens machined from the boundaries of the molded panel, delamination failure precipitates along planes where resin rich areas accumulate or where visible fiber bending occurs, therefore leading to questionable results.

Control specimens following ASTM D2344 recommendations are $w/t = 2$ and $l/t = 6$, where t is the laminate thickness, w represents coupon width and l is the coupon

length, given by the span plus the overhang. The ASTM specified span to thickness ratio is 4, but values of 6 and 8 are here also investigated for this particular composite system and stacking sequence to quantify the previously reported decrease in apparent strength with increase in s/t ratios. Nominal values for each dimension are given in [table II](#).

Since ASTM D2344 specifies all specimen dimensions relative to laminate thickness, the “Joshua” specimens are also machined with notch dimensions (depth and height, see [fig. 1](#)) multiple of laminate thickness. In particular, the notch depth to specimen width (d/w) ratios investigated are $1/6$, $1/5$, $1/4$, $1/3$ up to $7/16$, beyond which values the specimen integrity is prejudiced (the limit being $1/2$). The nominal values of notch height to laminate thickness (h/t) ratios covered are $1/10$ and $1/5$. To be noted is that specimen width is also related to laminate thickness.

The notching process is performed on a milling machine; the specimen is clamped on the long side opposite to the one being machined and the coupon is fed longitudinally to the end mill. While good control of notch depth can be achieved, since the feeding depth controls it, notch height h is controlled by end mill blade thickness, and availability was only $1/32$ ” (0.031 in or 0.794 mm) and $1/64$ ” (0.015 in or 0.397 mm).

The coupons are placed in a sliding roller three point-bending fixture [4] and tested to failure (Mean static failure load, MSFL) on an Instron 1123 electro-mechanical, double-screw test frame under displacement control. Other test Settings are crosshead feed rate of 0.05 in/min (1.27 mm/min) and 2 Hz sampling rate on IBM PC-type computer.

Fig. 1. Schematic of the Joshua specimen and three-point bend test configuration

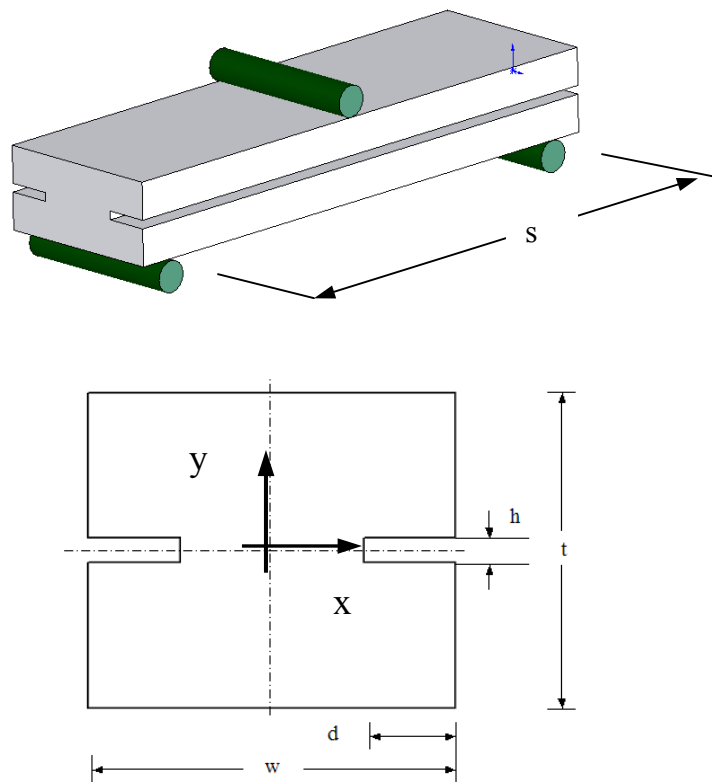


Table I. Unidirectional lamina and quasi-isotropic laminate elastic properties

E_1	E_2	G_{12}	ν_{12}
Msi (GPa)	Msi (GPa)	Msi (GPa)	
18 (124.10)	1.5 (10.34)	0.8 (5.51)	0.3

E_z, E_x	E_y	G_{xz}, G_{yx}	ν_{xy}, ν_{yx}
Msi (GPa)	Msi (GPa)	Msi (Gpa)	Msi (Gpa)
7.15 (49.29)	1.5 (10.34)	2.74 (18.89)	0.304

Table II. Summary of configurations tested: specimen geometry, test setup, and results.

Config. No.	s/t	d/w	h/t	Avg. P lb (N)	Avg. τ ksi (MPa)	sdev τ ksi (MPa)
1	4	0	0	632	10.98	0.23
2	4	1/4	1/10	517	16.28	0.15
3	4	1/4	1/5	502	16.70	0.23
4	4	1/6	1/10	539	13.45	0.44
5	4	1/6	1/5	608	14.39	0.03
6	4	1/6	1/8	457	14.25	0.73
7	4	1/5	1/5	221	7.69	0.14
8	4	1/4	1/5	N/a	N/a	N/a
9	4	1/3	1/5	216	9.87	0.42
10	4	7/16	1/5	164	14.88	1.09
11	6	0	0	482	8.69	0.03
12	6	1/4	1/10	354	12.37	0.33
13	6	1/4	1/5	401	14.04	1.48
14	6	1/6	1/10	372	11.37	N/a
15	6	1/6	1/5	448	11.78	0.39
16	6	7/16	1/5	104	9.29	1.50
17	8	0	0	452	7.78	N/a
18	8	1/5	1/10	358	10.82	0.37
19	8	1/4	1/10	332	11.92	0.18
20	8	1/3	1/10	226	12.64	0.63
21	8	1/6	1/10	351	9.92	N/a
22	8	7/16	1/10	77	7.73	0.88

2.2 EXPERIMENTAL RESULTS

In the ASTM D2344 coupon, onset of damage is characterized by a single crack that propagates from a region located about one thickness away from roller, usually at the axis of symmetry or within a $\frac{1}{4}$ of the thickness above. A sharp drop in the load-displacement curve and an audible cracking sound accompany catastrophic delamination, which is at times hard to detect without the aid of a microscope. After the first inter-ply failure, the load picks up again and in some cases it may reach the pristine value, see curve SBS in [fig. 2](#).

The various configurations of the Joshua specimen failed in a macroscopically “brittle” mode by sudden crack initiation and propagation. The load-displacement curves for four configurations tested, which are also plotted in [fig. 2](#), exhibit a much clearer, significant drop at the onset of damage, beyond which structural integrity of the coupon is compromised.

The delamination is generally more visible to the naked eye, and in the large majority of the specimens it is located near the vertical axis of symmetry, and right at the midplane, actually one ply above it. As previously reported [13], the highest fiber orientation angle mismatch appears to favor the path of self-consistent cracks such as delaminations ([fig. 3, 4](#)), as in the case of the interface between the 45 degree laminae of the present quasi-isotropic laminate, [...0/90/+45/-45//45/+45/90/0/...]. Furthermore, the lower bending stresses and compressive localized forces under the roller have less detrimental influence on the ILS stress profile, therefore allowing for a more pure state of shear stress to develop. However, in few of the specimens the delamination started at the location of first cross-sectional change, in the vicinity of the groove, thus, before changing planes and eventually reaching the same ± 45 interface in the proximity of the midplane. It was unfortunately not possible to rationalize between such specimens and notch characteristics or support configurations.

In general, the Joshua specimens failed at lower crosshead loads than the SBS ones, as anticipated due to the reduced area of delamination, and the average results are reported in [table II](#).

The structural stiffness for a simply supported beam loaded in the center is given by:

$$K = \frac{P}{\delta} = \frac{48EI}{L^3} \quad (1)$$

where P is the applied load, δ is the crosshead displacement, L is the support span, E the flexural modulus (since the homogeneous orthotropic assumption is invoked) and I the moment of inertia of the cross section.

For the short beam shear coupon, the latter is given by:

$$I_{rect} = \frac{wt^3}{12} \quad (2)$$

while for the Joshua specimen, which is basically an I-beam in nature, it is:

$$I_{1\text{beam}} = \frac{wt^3}{12} - \frac{2dh^3}{12} \quad (3)$$

Even considering ratios of $d/w = 3$ and $h/t = 1/5$, the difference in stiffness is barely 0.5%, therefore suggesting the adequacy of comparing L- δ curves.

Fig. 2. Load vs. displacement curves for the SBS and various Joshua specimens.

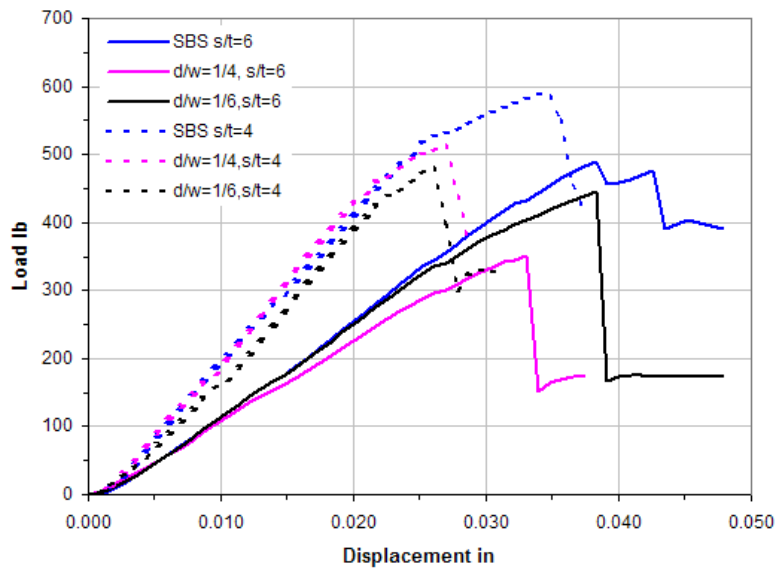
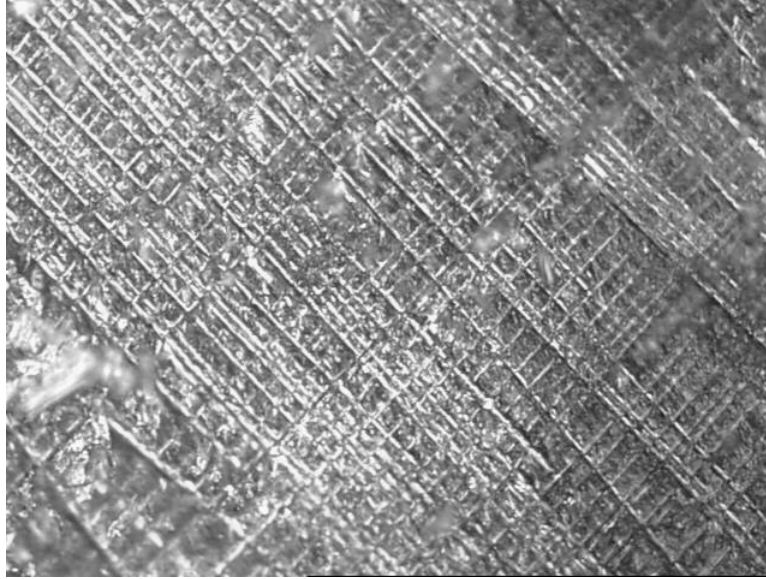


Fig. 3. Micrographic picture of cross-section of typical failed specimen.



.....
 0
 90
 +45
 -45
 -45
 +45
 90
 0

Fig. 4. The fracture (delaminated) surface shows the adjacent ± 45 laminae.



The measured values of ILS strength for the short beam and Joshua specimens are reported in table I. The variation of such results with the d/w and h/t ratios is plotted in [fig. 5](#) and [6](#), where the axis of ordinates corresponds to zero notch dimensions, which is the control SBS specimen. The three curves of [fig. 5](#) are qualitative indications of the trends observed for three values of s/t ratios, namely 4, 6 and 8. For each configuration it is possible to note that the introduction of the notch introduces an apparent increase in the measured strength, which highlights the fact that this test method fails to capture the true desired mechanical property.

However, it is possible to note that the results reach an asymptote for larger values of notch depth, until they reach the shaded area on the right where the results become unreliable since the specimen has lost integrity. The shaded area below indicates the regime of flexural rather than shear dominated failure, where again results cannot be considered valid. The beneficial presence of the notch appears to be counteracted by the compact geometry prescribed by ASTM of span to thickness ratio of 4. If, however, the flexibility of the specimen is increased to $s/t = 6$ and 8, it is possible to get even closer to the real value of ILS strength. Even though more work needs to be done, mainly to extend the results to greater s/t ratios, it appears that the correct regime where to investigate the true interlaminar shear strength is situated between values of $d/w = [0.3-0.4]$ and $s/t = [8-12]$.

On another front, it can be seen in [fig. 6](#) that notch height has little influence on the measured results. However, as a compromise between maintaining structural rigidity and alleviating eventual stress concentration, a value of $h/t = [1/10-1/5]$ is preferable. Post mortem inspection of the fracture surface, obtained by pulling apart the upper and lower halves of the specimen, revealed that notch depth varies notably along the specimen length, and can differ from the nominal value by a few percent. The inability to measure the actual value of notch depth by means of a traditional micrometer/caliper (the thickness of the blades being greater than the notch itself) requires the future activity to focus on developing a better machining procedure, thereby reducing the amount of scatter present in the data.

Fig. 5. The plot shows the variation of the measured ILS strength with the notch depth to specimen width ratio (d/w), for different values of span to thickness ratios.

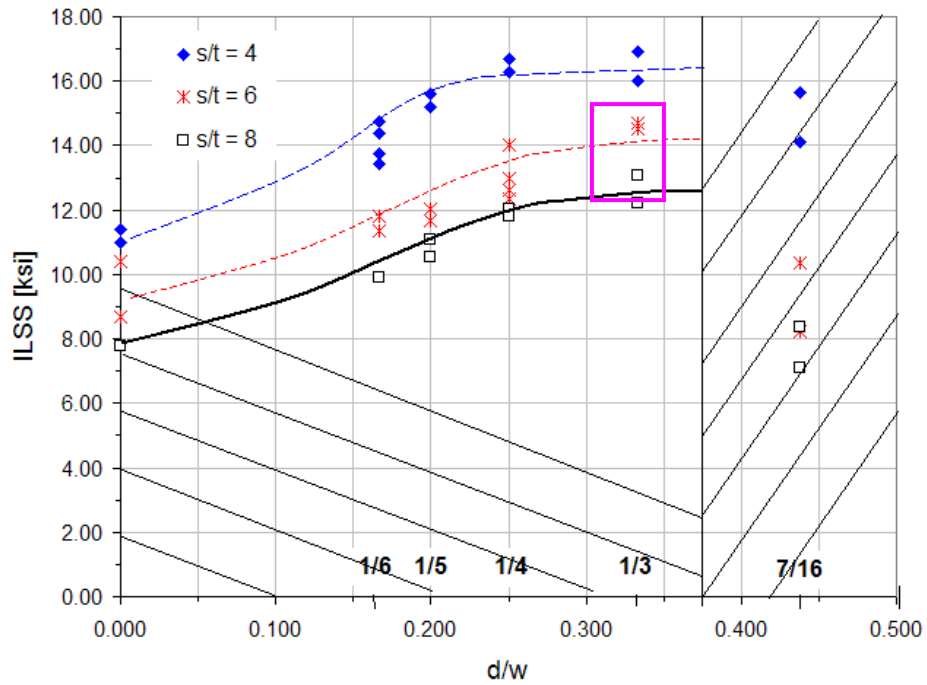
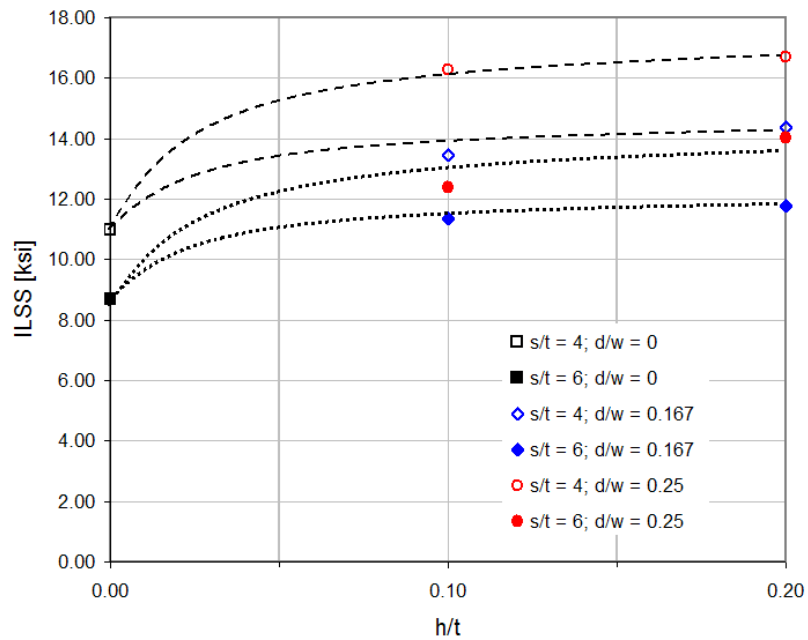


Fig. 6. The plot shows the variation of the measured ILS strength with the notch height to specimen thickness ratio (h/t), for different values of span to thickness ratios.



2.3 ANALYTICAL AND NUMERICAL RESULTS

The Joshua specimen can be interpreted as a modified I-beam, with very low slenderness ratio. The reduction in cross-area at the midplane introduces an abrupt increase in the interlaminar shear stress state of the specimen, which in turn precipitates failure at lower applied loads than the conventional SBS specimen. From beam theory, the load to failure increases linearly with the specimen width, hence, [fig. 1](#):

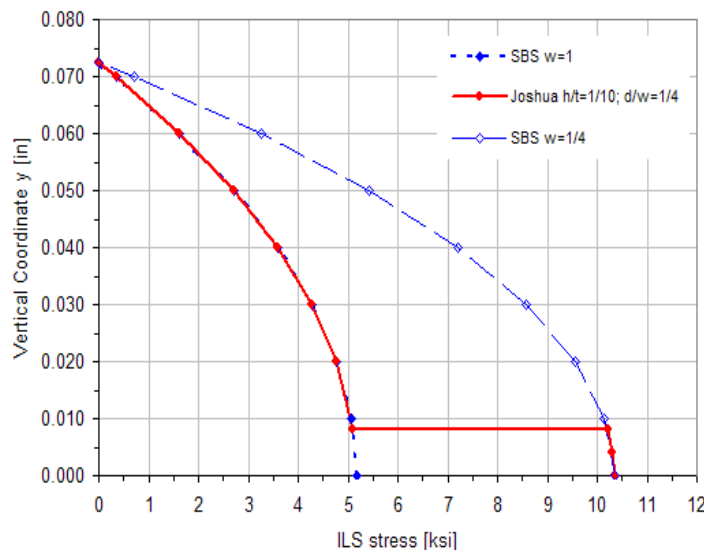
$$\tau = \frac{6V}{wt^3} \left(\frac{t^2}{4} - y^2 \right), y = [+t/2, -t/2] \quad (4)$$

where $V = P/2$. Eq. 4 describes the parabolic distribution of transverse shear stress in an isotropic beam, where y is the vertical coordinate. In relatively homogeneous composite laminates, such as the unidirectional prescribed by ASTM International or the present quasi-isotropic laminate, the value that is usually calculated is the peak ILS that theoretically occurs at the midplane:

$$\tau_{MAX} = \frac{3}{2} \frac{V}{wt}, \text{ for } y = 0 \quad (5)$$

However, the higher susceptibility for failure between the 0's and 45's in the case of $[0_n/\pm 45_m]_s$ laminates, the onset of delamination might occur at lower applied loads and be quite lower than the actual material strength, again confirming the strict dependence of the measured strength from test configuration. Due to the more sensitive nature of this test, it might be possible to extrapolate eventual differences in ILS strength due to laminate lay-up, undetectable with the SBS test [4].

Fig. 7. Plot of the ILS stress profile through the (half) thickness, for an applied load of 200 lb (890 N), for the SBS specimen and three Joshua specimens.



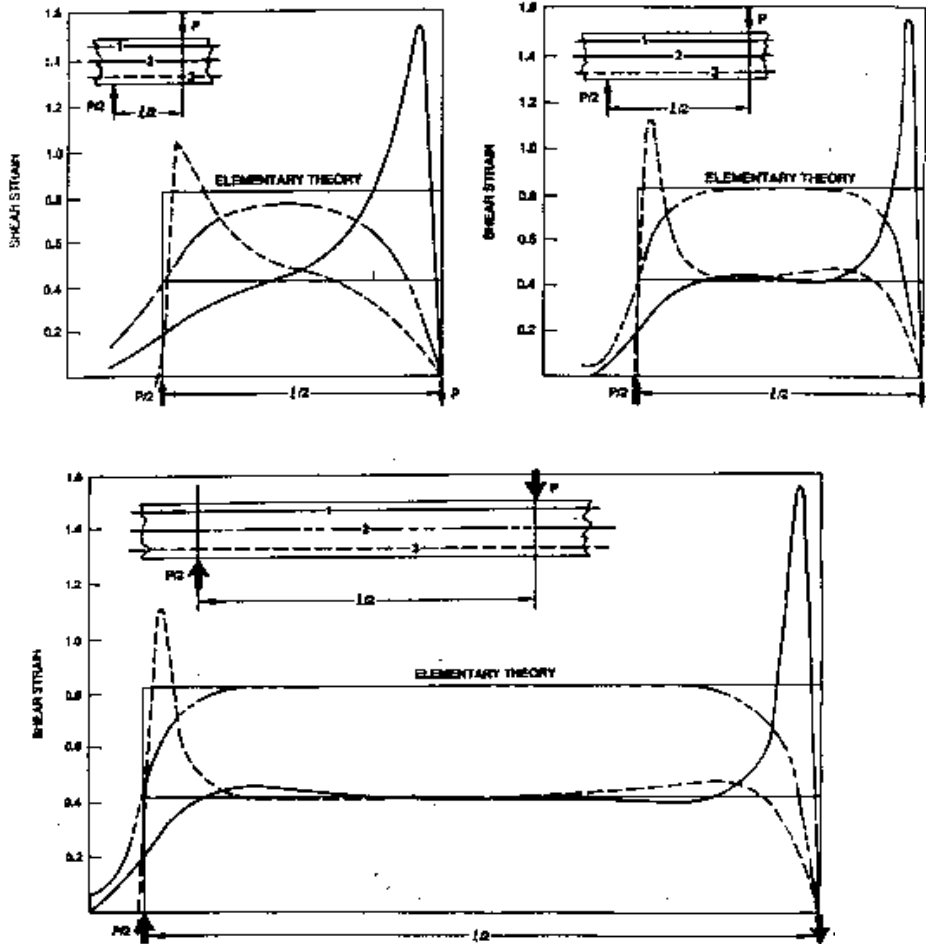
Plotted in [fig. 7](#) is the ILS stress distribution originating for a benchmark applied load, for two SBS specimens and a Joshua specimen with $h/t = 1/10$. Due to symmetry, only one half of the specimen is depicted, for $y = [t/2, 0]$. Of the SBS specimens, one has a width equal to the web width of the Joshua specimen; the other has a width equal to its flange width, therefore giving ideal lower and upper bounds for ILS stress distributions.

For the Joshua specimen, the shear distribution of an I-beam:

$$\tau = \frac{6V}{(w-d)t^3} \left(\frac{t^2}{4} - y^2 \right) \quad (6)$$

Previous research [4-12] has shown that the ILS stress distribution through the thickness obtained from beam theory is accurate in the range of 1 to 2 thicknesses away from the rollers, where the influence of contact forces on the stress profile diminishes. The ILS stress profiles along the length of the SBS specimen, at three different locations through the thickness and for three different s/t ratios, namely 3,6 and 12 are plotted in [fig. 8 a,b,c](#). It is possible to identify that a more uniform shear stress state can be achieved for specimens with higher s/t ratios, and its peak value is closer to the maximum value predicted by beam theory. Furthermore, such peak value is attained over a greater length, therefore allowing for a greater strain energy density to accumulate. From previous experience, it has been discovered that interlaminar failure is more likely to originate at locations of greater shear strain energy density, 1.5 thicknesses away from the loading roller, rather than in its proximity, where the compressive forces preclude the initiation and propagation of a crack. In the case of the Joshua specimen, the lower load required to induce failure in the thinner flange can be carried more easily by the larger webs.

Fig. 8 a, b, c. Shear strain distribution along interlaminar plane $s/t = 3, 6,$ and 12 .



A quarter model of the Joshua specimen is built with the aid of the commercial FE code ANSYS, whereby the use of symmetry boundary conditions reduces the computational effort. The model is similar to the one developed in [4]: the load is applied by means of concentrated nodal forces, and simply supported boundary conditions are supplied.

The model employs solid quadrilateral 8-node elements, with one element per ply for a total of 32 elements through the thickness, and 5 across the width. Macroscopic laminate (smeared) properties from table I are assigned as engineering constants rather than ply-by-ply, due to the fairly homogenous nature of the present lay-up. The Joshua specimen in question has dimensions: $d/w = 1/4$, $h/t = 1/10$, $s/t = 6$.

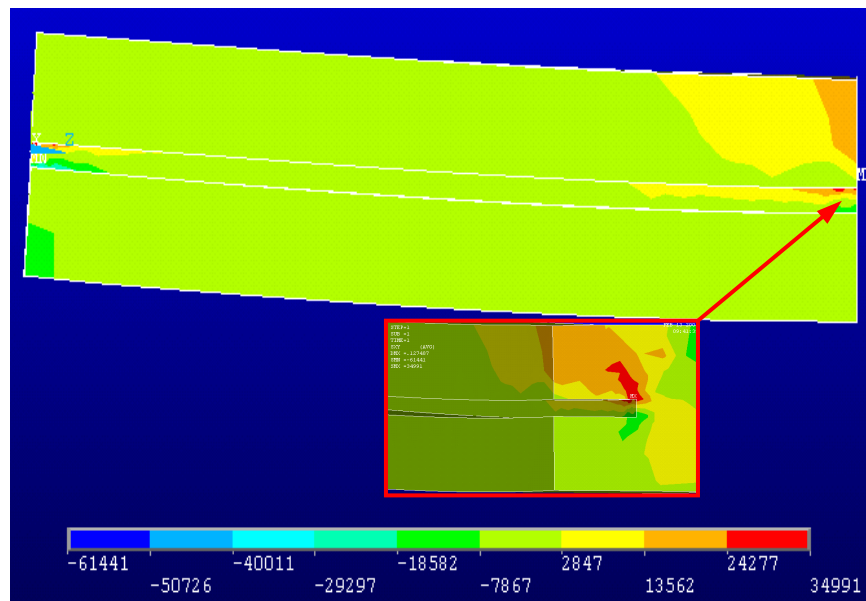
The ILS stress profile shown in fig. 9 qualitatively resembles the distribution found in [4], and the calculated value of peak stress in the area of reduced width away from the notch (13.56 ksi) is very close to the experimentally measured and estimated "true value" of [12.5-14] ksi.

However, a closer look at the region in the vicinity of the notch seem to suggest that the sudden change in cross section introduces a stress concentration in the vicinity of the notch, which in turn may originate the delamination.

As previously stated, few of the specimens exhibited such behavior, before the delamination could fully develop and reach the ± 45 interface in the proximity of the midplane.

It is possible that in the vicinity of the notch the yield strength of the neat resin is locally exceeded, and the crack thus nucleated might in turn develop into a delamination. Together with improving the machining procedure, future work will investigate whether notch shape (such as V-grooved or rounded end mill blades) might also contribute in achieving a better control over the location of failure initiation.

Fig. 9. ILS stress profile for the Joshua specimen along the length.



3. CONCLUSIONS

The effect of introducing a notch in the short beam shear (SBS) test specimen to reduce the area resisting the maximum interlaminar shear stress has been investigated. In the attempt to develop a test specimen, which is independent of test parameters, an investigation has been carried out analytically and experimentally to determine the influence, if any, of notch dimensions on the measured ILS strength of a carbon/epoxy laminates, and eventually establish an optimum configuration.

By reducing the width of the specimen around the midplane, therefore by precipitating failure at lower applied loads, the modified “I-beam” specimen, also known as Joshua specimen, has shown an ability to carry more satisfactorily the inherent bending stresses that originate due to the three-point configuration, hence allowing for employing a more flexible geometry while maintaining a shear dominated failure mechanism. While a better machining process methodology needs to be developed, and a more extensive database needs to be gathered to verify the general validity of these results for other material systems, stacking sequences, and test geometries, preliminary results seem to suggest that the Joshua

specimen can provide a viable alternative to existing test methods, finally allowing for the closer estimate of the true value of ILS strength.

ACKNOWLEDGMENTS

The authors would like to thank **Dan Jacobson** (C.G.Co.) for supplying the materials and providing support throughout the research. *Per aspera astra ad ulteriora.*

REFERENCES

1. T.K. O'Brien – Interlaminar shear fracture toughness, G_{IIc} : shear measurement or sheer myth? – 7th ASTM Symposium on Composite Materials: Fatigue and Fracture – 1997, also in: NASA TM 110280;
2. T.K. O'Brien – Interlaminar Fracture Toughness: The Long and Winding Road to Standardization – Composites Part B, 29B (1) – 1998;
3. ASTM D2344 – Apparent interlaminar shear strength of unidirectional parallel fiber composites by short beam method;
4. P. Feraboli, K. Kedward – Four-point bend interlaminar shear testing of uni- and multi-directional Carbon/Epoxy composite systems – Composites Part A, 34 (12) – 2003;
5. D. Adams, E. Lewis – Experimental study of Three and Four Point Shear test specimens – J. of Composites technology and Research, 17 (4) – ASTM 1995;
6. M. Xie, D. Adams – Study of Three and Four Point Shear testing of unidirectional composite materials – Composites, 26 (9) – 1995;
7. K. Kedward – On the short beam test method – Fibre Science and Technology (5) 1972 pp. 85-95;
8. J.M. Whitney, C.E. Browning – On short beam shear tests for composite materials – Experimental Mechanics, 25 (3) – 1985;
9. J.M. Whitney – Elasticity analysis of orthotropic beams under concentrated loads – Composites Science and Technology, 22 – 1985;
10. M.R. Wisnom – Modeling of stable and unstable fracture of short-beam shear specimens – Composites, 25 (6) – 1994;
11. F. Rosselli, M.H. Santare – Comparison of the short beam shear (SBS) and interlaminar shear device (ISD) – Composites Part A, 28A – 1997;
12. K. Shivakumar, F. Abali, A. Pora – Modified Short Beam Shear Test for measuring interlaminar shear strength of composites – Technical Note, AIAA Journal, 40 (11) – 2002;
13. P.J. Feraboli, D.R. Ireland, K.T. Kedward – On the role of Force, Energy and Stiffness in Low Velocity Impact events – 18th ASC Technical Conference – 2003.